A Method for Correcting FTS Dynamic Alignment Errors

M. W. Kelly & D. L. Mooney

SPIE
Defense and Security Symposium
April 14, 2004

This work was sponsored by the Department of the Air Force under Air Force Contract No. F19628-00-C-0002.
Opinions, interpretations, conclusions and recommendations are those of the author and are not necessarily endorsed by the United States Government.

Outline

- Background
- Modulation Efficiency and Dynamic Alignment Errors
- Correction of Raw Interferograms
- Correction of Decimated Interferograms
- Simulation of Correction on CrIS
- Summary

NPOESS is the Next Generation of Polar Environmental Satellites

- Near circular, sun-synchronous 833 km orbit
- 98.7 degree inclination
- 1330 (ascending) 0530 & 0930 (descending) nominal equatorial crossing times
- 10 year operational lifecycle
- 12 payloads
  - Down-looking atmospheric and terrestrial measurements
  - Space environment monitors
- Tri-agency partnership formed to to acquire, build, and operate satellites
  - DoD, DOC, NASA

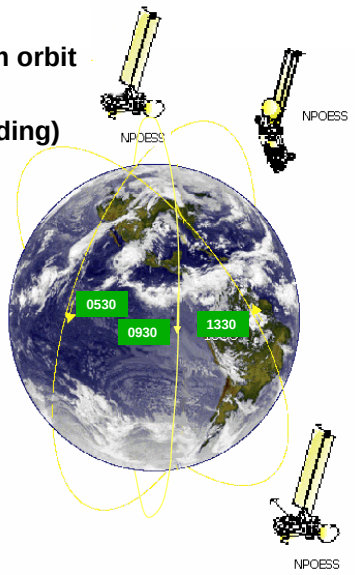

MIT Lincoln Laboratory

SPIE 2004 Orlando
3/5/2004

The National Polar-orbiting Environmental Satellite System was established by presidential order in 1994. NPOESS will fly as a two-satellite constellation, in a 833 km altitude, 98.7 degree inclination, sun synchronous orbit. There will be a 1330 and 1730 ascending equatorial crossings. The primary function is to collect meteorological data.

NPOESS is managed by the Integrated Program Office, which is a new agency within NOAA. The IPO was formed as a tri-agency partnership between the DoD, NOAA, and NASA. The DoD is responsible for the acquisition of new sensors and launch support. NOAA is responsible for system operations. NASA is developing an implementing new technologies into NPOESS.

Cross-track IR Sounder (CrIS)

- **High spectral resolution measurements of Earth's radiance to determine the vertical distribution of temperature, moisture, and pressure in the atmosphere**
- **Contractor: ITT Industries Ft. Wayne**

Michelson Interferometer

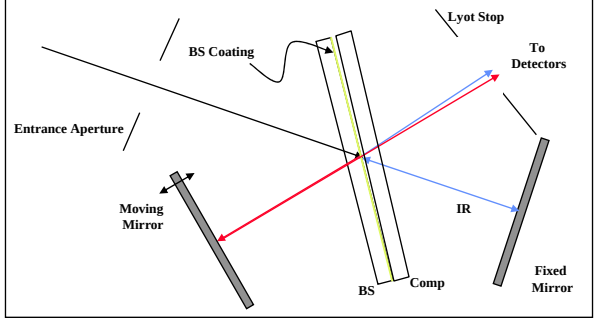

Modulated Interferogram

$$I(z) = c\int_0^\infty S(u)ME(u,z)\cos(2\pi zu)du$$

$$c = \frac{1}{2}A\Omega\tau\rho G_A$$

$$S(u) = B(u)F(u)H(u)$$

MIT Lincoln Laboratory

SPIE 2004 Orlando
3/5/2004

CrIS is the IR sounder portion of the cross-track IR-microwave sounding suite (CrIMSS). It is a FTS which collects high resolution spectral data between approximately 3 – 15 microns. ITT was selected to build CrIS.

The Michelson interferometer within the spectrometer modulates input radiation at a frequency equal to the product of the wavenumber of the radiation and the constant optical path difference (OPD) velocity associated with the moving mirror. The modulation efficiency depends on the angular alignment of the two wavefronts exiting the spectrometer

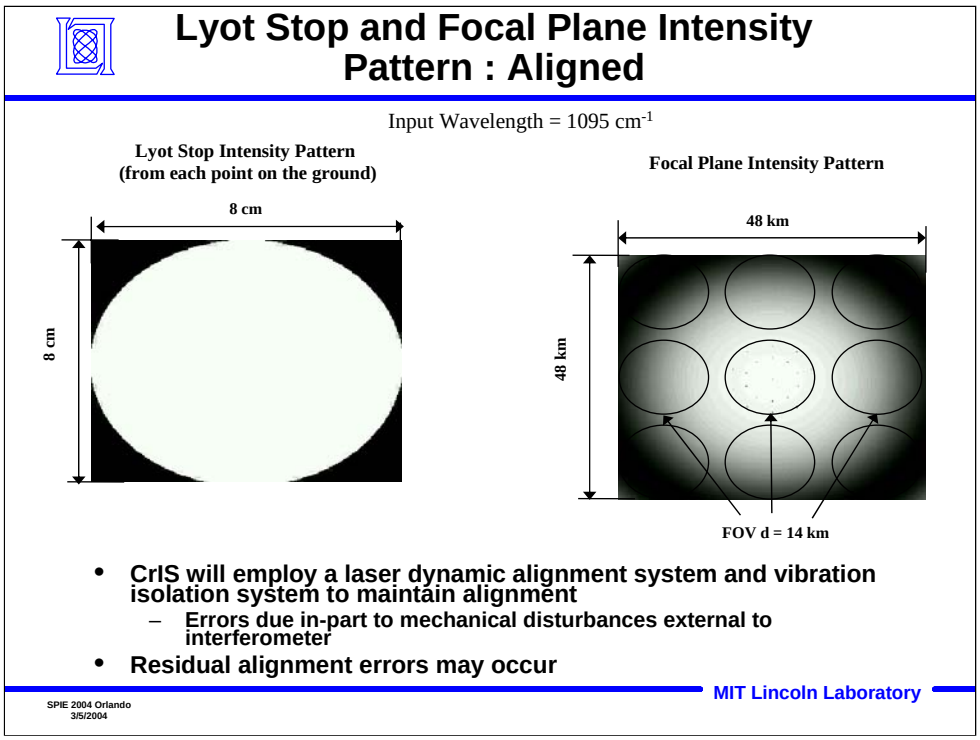

Pictures show the lyot stop in the interferometer and the image at the focal plane when aligned.

Mechanical disturbances can cause errors in the alignment of the wavefronts which manifest as noise in the spectrum. To mitigate these affects CrIS will employ a laser to monitor alignment and dynamically correct the errors. Additionally, a vibration isolation system will damp disturbances imparted to the sensor from the spacecraft. Despite these efforts, residual noise may remain under certain conditions.

Interferometer Dynamic Alignment Errors Create Noise in Spectrum

- **A misalignment reduces the modulation efficiency by:**

$$ME(u) = \frac{2J_1(2\pi u a \theta)}{2\pi u a \theta}$$

J_1 = Bessel Function of the First Kind
a = Lyot Stop Radius
u = Wavenumber
θ = Wavefront Tilt Angle

- **Multiplicative interferogram error due to DA errors is proportional to the slope of the ME curve evaluated at the bias angle**
  - **Slope of Bessel function increases with a tilt bias**

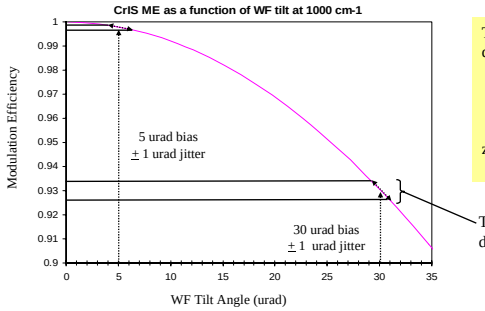

The interferometer output intensity amplitude depends on ME

$$I(u,z) \sim ME(u,z) \cdot B(u)[1-\cos(2\pi u z)]$$

z - Optical path difference between the interfering wavefronts

The output intensity amplitude varies more due to alignment jitter when a large bias exists

SPIE 2004 Orlando
3/5/2004

When a static alignment error exists, the interferometer is much more sensitive to jitter. The figure shows how the modulation varies with a 2.5 urad peak to peak dynamic jitter. With a large offset, the modulation is down on the bessel function curve, and the small perturbation causes a relatively large change in modulation. Comparatively, with a small offset the modulation is on a flat part of the curve, and is not sensitive to dynamic jitter.

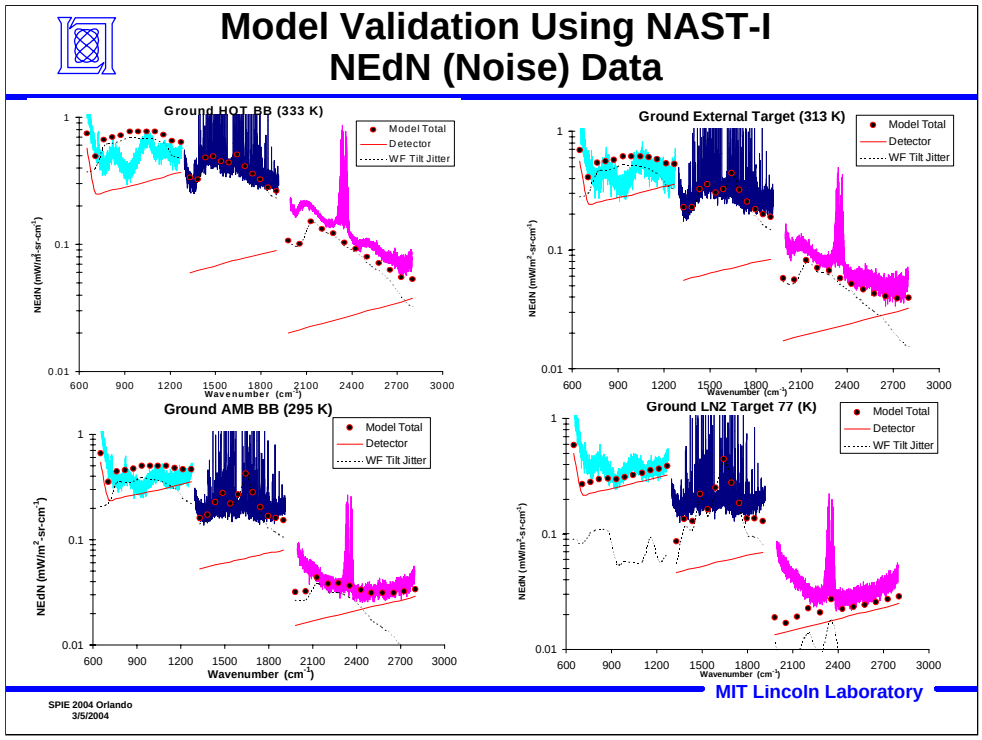

The NAST platform is airborne with many vibrational disturbances including coolers for detectors, heaters for the optical bench, aircraft engines, ….

Although the DA system removes most of the disturbances, some jitter remains both in flight and on the ground.

On the ground, where the jitter power spectrum is known precisely, a comparison between model and measurement is even more favorable. Both detector and jitter noise contributes to the total system noise. The LN2 scene was difficult to model. Room temperature radiation reflected from the liquid surface, dewar, and possibly water vapor in the dewar make modeling the scene flux difficult. Given those conditions, the model comparison with the data is quite good.

Estimate of the Jitter Induced Interferogram Error Term

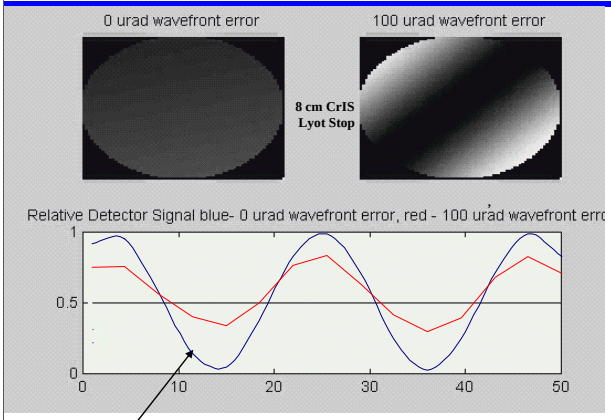

Detector Detects Total Integrated Intensity at Lyot Stop

Measured Interferogram is Error-free Interferogram Plus Error Term

$$I(z) = I_o(z) + \delta I(z)$$

Error Term Estimate For Small Misalignments (< ~20 urad)

$$\delta I(z) \approx -c \frac{[\pi a \theta(z)]^2}{2} \int_0^\infty S(u) u^2 \cos(2\pi z u) du$$

MIT Lincoln Laboratory

SPIE 2004 Orlando
3/5/2004

The modulated interferogram can be written in terms of the error free interferogram, Io(z), plus an error term dI(z).

The objective of this work is to recover Io(z) given I(z) and b(z), i.e, determine dI(z) and add it to I(z).

The plot shows how the intensity varies at the lyot stop and focal plane when DA jitter is present.

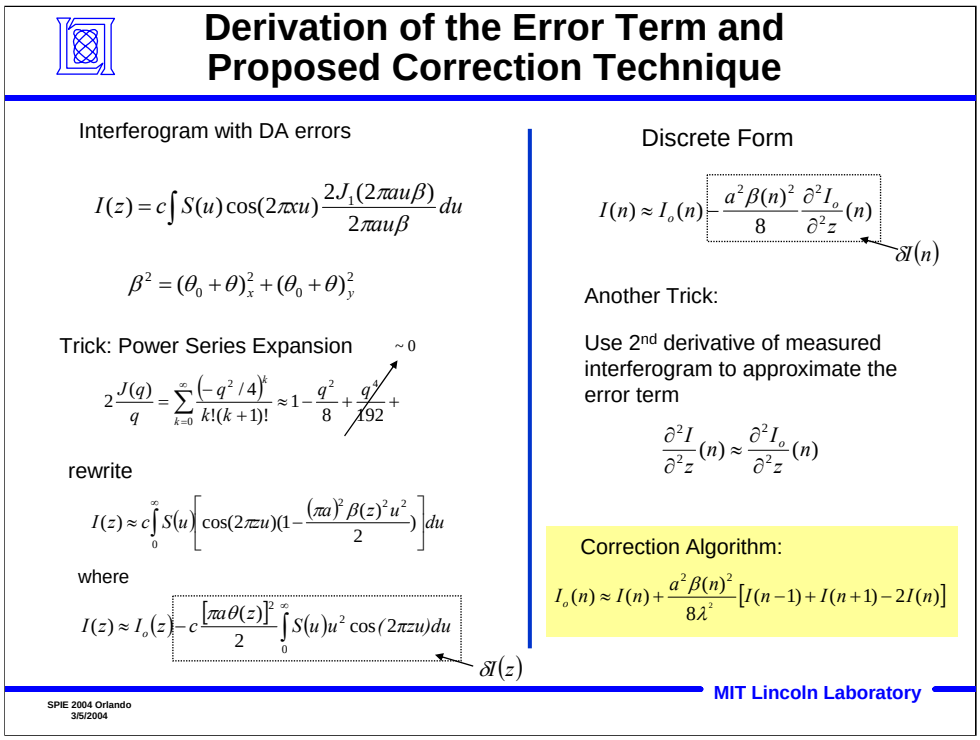

To derive the correction first expand the ME bessel function into a power series.

Then the DA error at each point in the spectrum is proportional to the angle b(z) multiplied by the second derivative of the discrete, error free interferogram, Io''(z). The measured, discrete interferogram can be formally written in terms of the second derivative of Io.

The correction algorithm uses a numerical second derivative technique

Simulation of CrIS Interferograms and Jitter Correction Algorithms

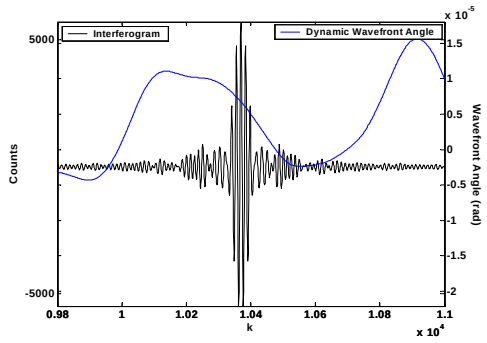

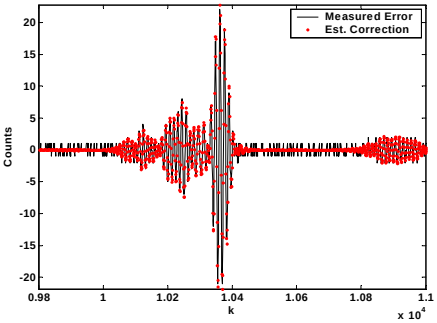

- **Black- simulated interferogram**
  - **Includes the effects of self-apodization, photon shot noise, electronics noise, non-linearity, optical dispersion, background flux, ghosts, and 1/f noise**
- **Blue- Dynamic alignment error**

- **Black- difference of error-free interferogram and corrupted interferogram**
- **Red – estimated correction using the numerical second derivative of corrupt signal**

Slide shows the correction for the case of 250 Hz band-limited jitter centered at baseband. The "measured" error (black line) is determined by differencing the corrupted interferogram with a jitter-free interferogram. The correction (red points), calculated using equation discussed on the last slid is also plotted, showing a good match. The plot is shown around the interferogram peak, where the error is the greatest. The correction far away from the peak, and where the wavefront alignment is good, is small compared with the noise.

Operationally CrIS Interferograms are Decimated for Communication

- **Raw interferograms and spectra (A&B) are decimated (C&D) for transmission to the ground**

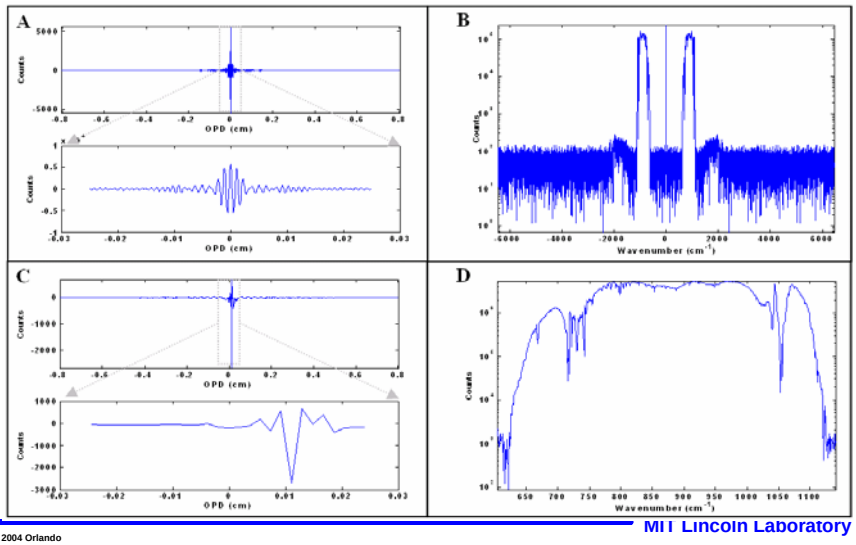

In this work, we simulated LW band interferograms, several mechanical disturbance scenarios, and correction performance for three possible implementations. This slide shows the simulated raw A&B and decimated C&D interferograms and the associated spectra. The scene radiance used to generate the interferograms was simulated from mid-latitude TIGR data. The spectra are calculated directly by Fast Fourier Transforms (FFTs) of the simulated interferograms. In each case the appropriate shift was applied to the spectra for presentation.

Two Techniques to Correct Decimated Data

Up-sample to recover an Estimate of Un-decimated Interferogram

$$I_{us}(nK) = KI_d(n), \quad L-1 < n > 0$$
$$I_{us}(n) = 0, \quad otherwise$$

$$\hat{S}(k) = W(k)\frac{1}{N}\sum_{n=0}^{N-1} I_{us}(n) e^{-i2\pi\frac{nk}{N}}$$

$$I(n) \approx \hat{I}(n) = \frac{2}{N} \cdot real\left[\sum_{k=0}^{N-1}\hat{S}(k)\sum_{j=0}^{N-1} b^{-1}(j) e^{i2\pi\frac{(n-j)k}{N}}\right]$$

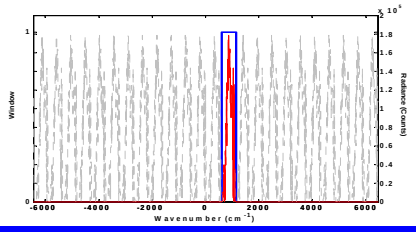

Calculate Analytical Derivative Directly on Decimated Interferogram

$$\frac{d^2 I_d}{dx^2}(n) = \sum_{k=0}^{M-1} S_d''(k) e^{i2\pi\frac{nk}{M}}$$

$$S_d''(k) = \sum_{j=0}^{K-1}\left(i2\pi\frac{k+j\cdot L}{N}\right)^2 S_b(k+j\cdot L)$$

$$I_{o,d}(n) \approx I_d(n) - \frac{(\pi a)^2 \beta(nK - N_f/2)^2}{8}\frac{\partial^2 I_d(n)}{\partial^2 z}$$

$\delta I_d(n)$

Assumes low frequency alignment errors < ~250 Hz

Two methods for calculating the correction on decimated interferograms were explored, recovering an estimate of the raw interferogram to compute the numerical second derivative, and computing it analytically directly on the under-sampled data. After the up-sampled interferogram is recovered, the correction technique discussed earlier is applied.

The analytical technique is much less computationally intense, but only functions well with low-frequency jitter, less than about 250 Hz.

Simulation of Decimated Interferograms and Jitter Correction Algorithms

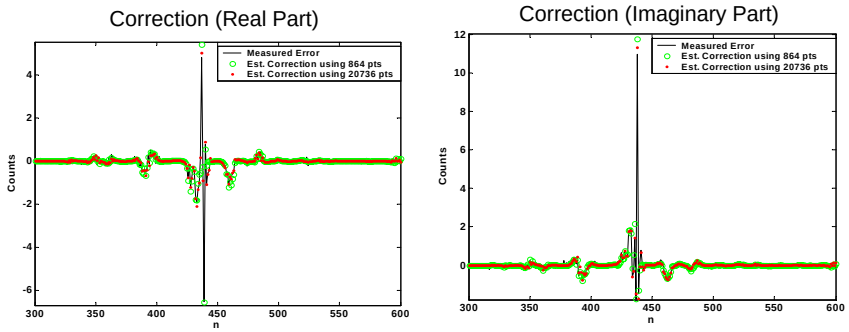

- **Black- difference of error-free, decimated interferogram and corrupted, decimated interferogram**
- **Red – estimated correction using the numerical second derivative on up-sampled & windowed interferogram**
- **Green - estimated correction using the analytical second derivative on decimated interferogra**

This slide shows an example of the real and imaginary decimated corrections for the case of 250 Hz band-limited jitter centered at baseband, compared to the "measured" error (black line) for both correction methods discussed above. The "measured" error was computed by differencing the corrupted, decimated interferogram with a jitter-free, decimated interferogram in the simulation. The correction calculated by up-sampling the corrupted interferogram and angles, and then decimating the results is plotted in red (points). The correction calculated directly on the decimated interferogram and angles is plotted in green (circles). Both compare favorably to the measured error with a small difference at the peak.

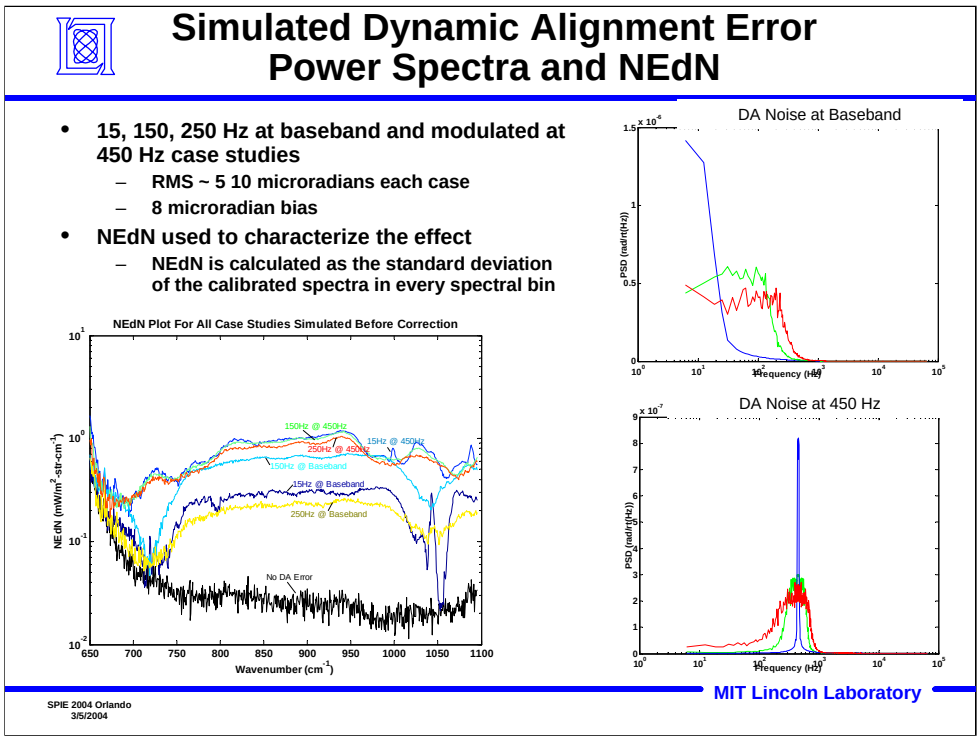

Six mechanical disturbance cases were considered in this work. The DA wavefront power spectra for each scenario are shown. Power spectra centered at baseband were derived by low-pass filtering a random error with a 4-pole Butterworth filter. The -3 dB cutoff was set to 15 Hz, 150 Hz, and 250 Hz. The band-limited spectra were then modulated at 450 Hz to simulate a tone. The RMS error for each case was approximately 5-10x10-6 radians. In addition to the dynamic error, an 8x10-6 radian static error was simulated. Simulated angle data were noise-free and quantized between 6- and 12-bits to model down-linked data. All computations were 64-bit floating point operations.

The noise equivalent delta radiance is shown plotted for the case when no error is present (black) and each of the jitter power spectra

Dynamic Alignment Error Noise is Highly Correlated

- **Use graphical noise correlation matrix as an indicator of dominant source of noise**
- **Detector & electronics noise floor is uncorrelated (random from one spectral bin to the another)**
- **Dynamic alignment errors produce correlated noise (erroneous signal appears in multiple spectral bins)**

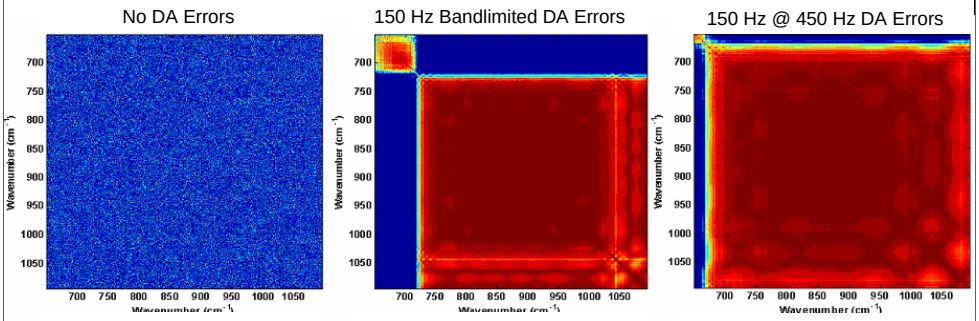

SPIE 2004 Orlando
3/5/2004

MIT Lincoln Laboratory

the noise correlation matrix was calculated to determine the mechanism of the dominant noise source in each spectral bin. Unlike detector or electronics noise, which in general are uncorrelated, dynamic alignment jitter noise is highly correlated from channel to channel.

This slide shows a graphical representation of the noise correlation matrix for three case studies: No DA jitter, 150 Hz Baseband jitter, and 150 Hz jitter modulated at 450 Hz. In each case, the matrix diagonal is identically one (deep red). Random noise is completely uncorrelated between channels and, if dominant, the matrix value is zero (deep blue). DA jitter noise is highly correlated and, if dominant, the matrix value is one (deep red). Dynamic alignment errors are dominant throughout most of the spectrum when not corrected.

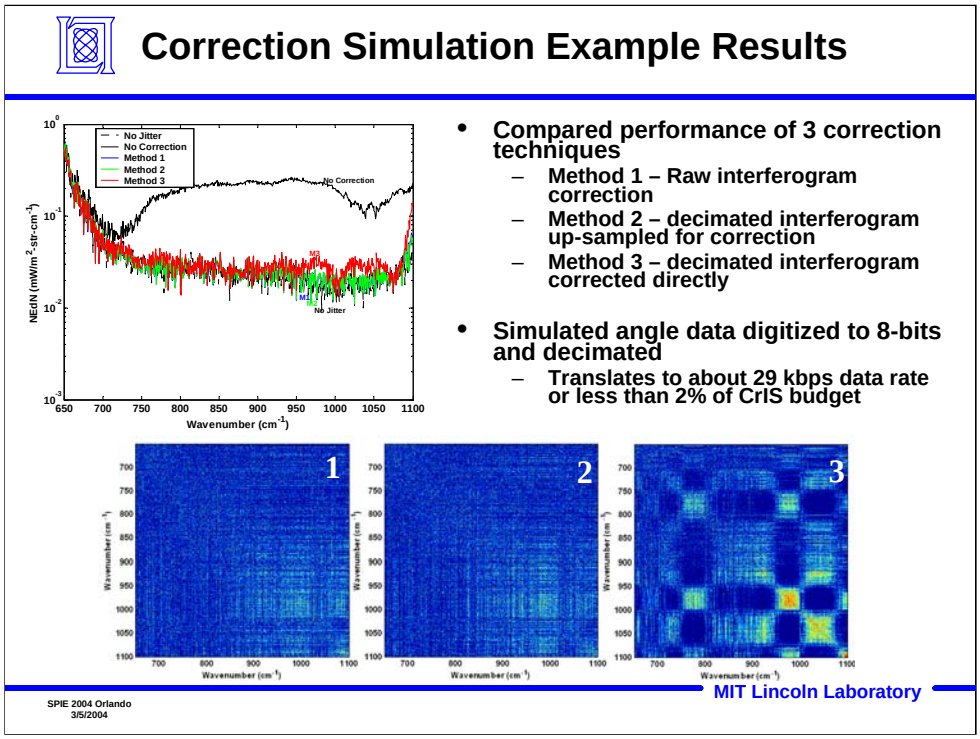

Correction Method 1 refers to the correction before decimation. Correction Method 2 refers to the technique after decimation and up-sampling the spectrum to use a numerical second derivative. Correction Method 3 refers to the technique after decimation and calculating the second derivative analytically on the down-sampled interferogram

This slide shows the NEdN of interferograms corrupted with 250 Hz band-limited jitter at baseband before correction (black solid) after correction Method 1 (blue), after correction Method 2 (green), and after correction Method 3 (red). Also plotted is the NEdN of jitter-free interferograms (black dotted). The corrections all reduce the noise down to the jitter-free case. There is a small increase in noise around 950 – 1050 cm-1 when Method 3 was used.

Also shown are the graphical representation of the noise correlation matrix for each correction method. Some areas of strong noise correlation exist between 950 and 1100 cm-1 when Method 3 is used to correct jitter errors. All other regions for all three methods are uncorrelated, indicating the correction reduced the errors below the detector/electronics (white) noise floor.

DA Correction Simulation Results

- **Digitized angles to 6- 8- 10- and 12-bits**
- **Results evaluated on *mean* NEdN reeducation and *mean* correlation matrix**
  - **Approximately factor of 10 reduction in noise achievable even with decimated interferograms**
  - **Low frequency DA noise reduced down to random noise floor**

		Mean NEdN Ratio						Mean Correlation					
	Jitter PSD	15Hz @ 0Hz	15Hz @ 450Hz	150Hz @ 0Hz	150Hz @ 450Hz	250Hz @ 0Hz	250Hz @ 450Hz	15Hz @ 0Hz	15Hz @ 450Hz	150Hz @ 0Hz	150Hz @ 450Hz	250Hz @ 0Hz	250Hz @ 450Hz
	No Jitter	1.00	1.00	1.00	1.00	1.00	1.00	0.00	0.00	0.00	0.00	0.00	0.00
	No Correction	8.20	26.88	17.78	26.11	6.59	23.84	0.48	0.83	0.48	0.85	0.51	0.86
6 bit Angle Digitization	Method 1	1.50	3.19	1.97	3.51	1.23	3.53	0.33	0.61	0.44	0.64	0.10	0.70
	Method 2	1.51	3.14	1.99	3.46	1.23	3.49	0.33	0.61	0.44	0.65	0.10	0.70
	Method 3	1.56	6.94	2.21	6.73	1.79	6.31	0.31	0.19	0.43	0.17	0.12	0.20
8 bit Angle Digitization	Method 1	1.10	2.82	1.49	2.86	1.13	2.85	0.07	0.56	0.32	0.52	0.03	0.54
	Method 2	1.11	2.78	1.51	2.81	1.14	2.81	0.07	0.56	0.32	0.53	0.03	0.54
	Method 3	1.10	6.87	1.69	6.64	1.66	6.27	0.04	0.14	0.21	0.14	0.02	0.12
10 bit Angle Digitization	Method 1	1.11	2.74	1.42	2.74	1.17	2.73	0.08	0.53	0.30	0.49	0.07	0.50
	Method 2	1.12	2.69	1.44	2.69	1.17	2.70	0.08	0.54	0.30	0.49	0.07	0.50
	Method 3	1.11	6.85	1.63	6.64	1.69	6.28	0.07	0.13	0.15	0.13	0.04	0.12
12 bit Angle Digitization	Method 1	1.13	2.72	1.41	2.71	1.18	2.71	0.09	0.53	0.29	0.48	0.08	0.50
	Method 2	1.14	2.67	1.43	2.66	1.18	2.67	0.09	0.53	0.29	0.48	0.08	0.50
	Method 3	1.12	6.86	1.63	6.64	1.70	6.28	0.09	0.13	0.15	0.13	0.05	0.11

The results indicate very good correction results in all cases, between 4- and 12-times noise reduction. When the noise was confined to baseband the corrections were able to get within a factor of two of the jitter-free noise when angles were digitized with 8- or more bits. There was a slight fall-off when 6-bit resolution was used. When a tone was simulated, the correction still reduced the noise by about a factor of ten, but only achieved the noise floor to within a factor of approximately three. Again, digitizing with more than 6-bits produced slightly better results. As expected, Method 3 had more difficulty with the higher frequency jitter cases.

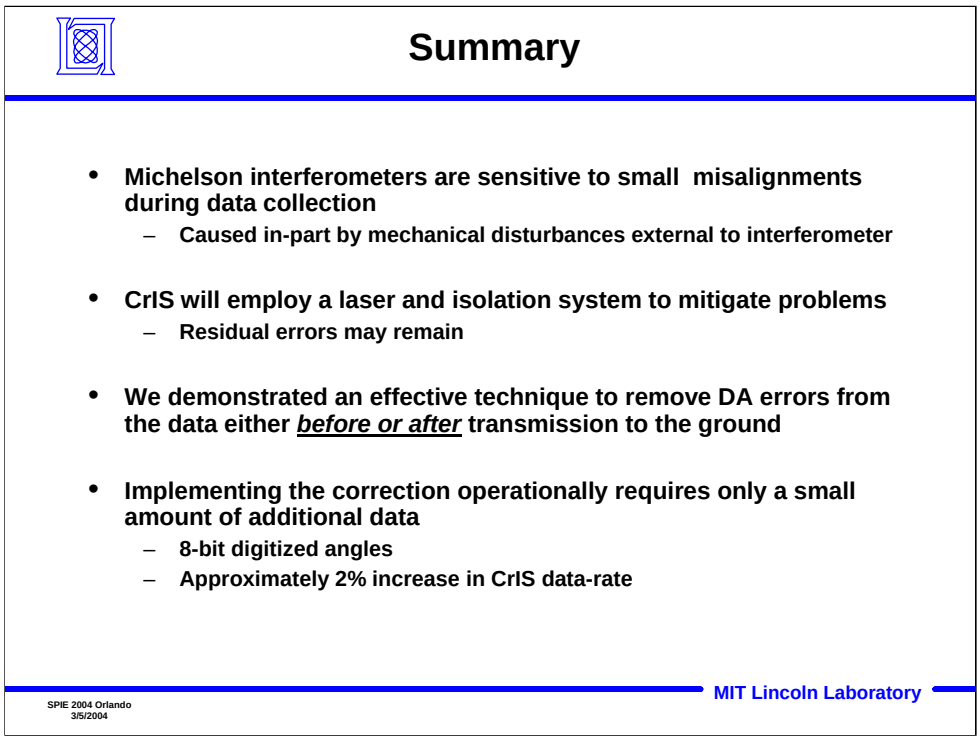

The Michelson interferometer within CrIS modulates input radiation at a frequency equal to the product of the wavenumber of the radiation and the constant optical path difference (OPD) velocity associated with the moving mirror. The modulation efficiency depends on the angular alignment of the two wavefronts exiting the spectrometer.

Mechanical disturbances can cause errors in the alignment of the wavefronts which manifest as noise in the spectrum. To mitigate these affects CrIS will employ a laser to monitor alignment and dynamically correct the errors. Additionally, a vibration isolation system will damp disturbances imparted to the sensor from the spacecraft. Despite these efforts, residual noise may remain under certain conditions.

Through simulation of CrIS data, we demonstrated an algorithmic technique to correct residual dynamic alignment errors. The technique requires only the time-dependent wavefront angle, sampled coincidentally with the interferogram, and the second derivative of the erroneous interferogram as inputs to compute the correction. The technique can function with raw interferograms on board the spacecraft, or with decimated interferograms on the ground. We were able to reduce the dynamic alignment noise by approximately a factor of ten in both cases.

Performing the correction on the ground would require an increase in data rate of 1-2% over what is currently planned, in the form of 8-bit digitized angle data.